

# Covalently Patterned Graphene Surfaces by a Force-Accelerated Diels–Alder Reaction

Shudan Bian,<sup>†</sup> Amy M. Scott,<sup>†</sup> Yang Cao,<sup>‡</sup> Yong Liang,<sup>‡</sup> Sílvia Osuna,<sup>‡</sup> K. N. Houk,<sup>\*,‡</sup> and Adam B. Braunschweig<sup>\*,†</sup>

<sup>†</sup>Department of Chemistry, University of Miami, Coral Gables, Florida 33146, United States

<sup>‡</sup>Department of Chemistry and Biochemistry, University of California, Los Angeles, Los Angeles, California 90095, United States

**S** Supporting Information

**ABSTRACT:** Cyclopentadienes (CPs) with Raman and electrochemically active tags were patterned covalently onto graphene surfaces using force-accelerated Diels–Alder (DA) reactions that were induced by an array of elastomeric tips mounted onto the piezoelectric actuators of an atomic force microscope. These force-accelerated cycloadditions are a feasible route to locally alter the chemical composition of graphene defects and edge sites under ambient atmosphere and temperature over large areas ( $\sim 1 \text{ cm}^2$ ).

Graphene has become the focus of much research attention because of its high conductivity, 2D structure, and superior mechanical properties.<sup>1</sup> Patterning onto the basal plane of graphene may increase the bandgap of graphene, a boon for integrated optics and electronics, or for the fabrication of graphene-based sensors.<sup>2</sup> However, a consequence of the stabilizing  $\pi$ -conjugation of graphene is that the basal plane is resistant toward chemical functionalization; thus, carrying out organic chemistry on graphene site-specifically is particularly challenging. Scalable methods to covalently pattern organic molecules onto graphene have not, to the best of our knowledge, been demonstrated. Functional molecules have been anchored to graphene using noncovalent interactions<sup>3</sup> or bonding to oxidized defect sites and edges.<sup>2d,4</sup> Alternatively, photochemical,<sup>5</sup> dipolar-cycloadditions,<sup>6</sup> and diazonium salt<sup>2b,7</sup> reactions couple organics directly with the basal plane of graphene, albeit not in patterns and with an input of energy that would denature or destroy soft matter. The recent report by Haddon et al. proposing that single layer graphene (SLG) participates in DA reactions as a dienophile at temperatures as low as 50 °C over 3 h<sup>8</sup> suggested to us conditions that could be used to scalably pattern graphene at ambient temperatures and atmosphere. Because of their negative activation volumes,<sup>9</sup> cycloaddition reactions are significantly accelerated in pressurized reaction vessels, and the Reinhoudt and Ravoo groups have covalently micropatterned various surfaces by inducing Cu<sup>1</sup>-free Huisgen and DA reactions through applied force between inked elastomeric stamps and surfaces.<sup>10</sup> Thus, we reasoned that a localized force exerted between SLG and a diene would accelerate the DA reactions and thereby immobilize molecules into patterns onto the basal plane of graphene through the formation of two new C–C bonds (Figure 1a).

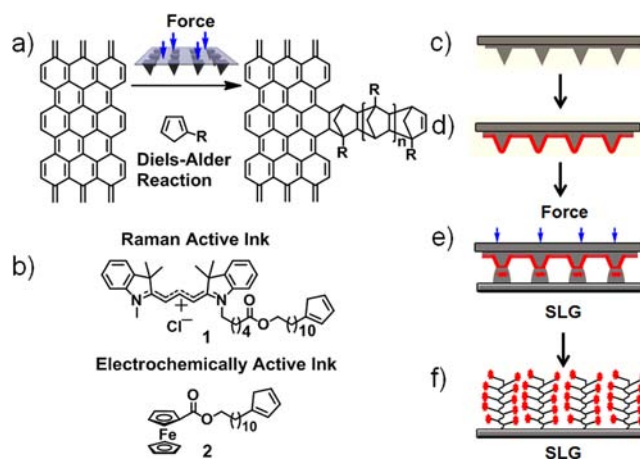


**Figure 1.** (a) DA oligomerization reaction between functionalized CP and a SLG surface. (b) Cy3-containing Raman active 1 and ferrocene-containing electrochemically active 2 ink molecules used to confirm force-accelerated patterning. (c) An elastomeric tip-array. (d) The tip-array coated with an ink mixture (red) consisting of a CP and poly(ethylene glycol) (PEG). (e) The inked tip array is pushed into the SLG surface. (f) Following rinsing of the surface to remove the PEG and excess CP, only the covalently immobilized molecules remain on the surface.

To demonstrate that force-accelerated cycloadditions could covalently pattern large areas ( $\sim 1 \text{ cm}^2$ ) of SLG sheets, we used an elastomeric tip array mounted onto the piezoelectric actuators of an atomic force microscope (AFM) to exert a localized force between functionalized CPs and SLG sheets. These tip arrays are commonly used for polymer pen lithography,<sup>11</sup> where patterns are formed by ink transfer from the tips to the surface through an aqueous meniscus. Moreover, their large areas ( $>1 \text{ cm}^2$ ) and the computer-controlled movement of the piezoactuators that hold the array provide high throughput and flexible pattern design. We have recently induced both the Cu<sup>1</sup>-catalyzed azide–alkyne click reaction<sup>12</sup> and the Staudinger ligation<sup>13</sup> on Au and SiO<sub>2</sub> surfaces with these tip arrays under ambient temperatures and pressures, confirming the suitability of these tip arrays for covalently immobilizing soft matter nondestructively through selective organic transformations. Because the elastomeric tips also

Received: August 1, 2012

Published: June 11, 2013

compress upon contact with surfaces, they can apply a predictable force between molecular inks and a surface,<sup>14</sup> so that in this experiment, the position, force, and reaction time can all be controlled precisely to pattern surfaces over cm<sup>2</sup> areas with micrometer-scale features.

Raman-active cyanine 3 (Cy3) containing CP **1** and electrochemically active ferrocene CP **2** (Figure 1b) were designed to characterize the bonding upon cycloaddition between the SLG surface and the CPs. CPs react quickly in DA reactions because of their geometric preorganization, and as a result, they have been utilized already in the context of surface patterning.<sup>15</sup> The Haddon group<sup>8a</sup> used Raman spectroscopy to follow a DA reaction on graphene and found that the D band at 1324 cm<sup>-1</sup> that corresponds to the A<sub>1g</sub> breathing vibration of sp<sup>2</sup> carbon rings, which is suppressed in pure graphene, increases significantly because the introduction of defects or covalently adsorbed molecules reduces the symmetry of the graphene lattice. The ratio of the D- and G-band integrations ( $I_D/I_G$ ) is a measure of the degree of functionalization of graphene.<sup>16</sup> Alternatively, electrochemistry can confirm the immobilization of the ink onto the surface and quantify the density of surface-bound molecules.<sup>12,17</sup>

Molecules **1** and **2** were synthesized and characterized by <sup>1</sup>H NMR, <sup>13</sup>C NMR, and high-resolution mass spectrometry, and all analytical data were consistent with the proposed structures.<sup>18</sup> The 8500 tip PDMS arrays with a tip-to-tip spacing of 80 or 160 μm were prepared following previously published literature protocols.<sup>11</sup> To induce the DA reaction between **1** and the SLG surface, **1** (0.8 mg, 1.2 mmol) and poly(ethylene glycol) (PEG) (2000 g mol<sup>-1</sup>, 10 mg mL<sup>-1</sup>) in 0.8 mL of 60:20 THF/H<sub>2</sub>O, which was sonicated to ensure solution homogeneity, were spin-coated (2000 rpm, 2 min) onto a tip array. The PEG matrix that encapsulates the CPs ensures even distribution of ink across the tip array, and ink transport from the tips to a surface is predictable and reproducible.<sup>12</sup> The tips were mounted onto the z-piezo of an AFM that was specially equipped with an apparatus to hold the tip arrays, an environmental chamber to regulate the humidity, and customized lithography software to control the position, force, and dwell-time of the tips (Figure 1c).<sup>18</sup> A 2 × 3 dot pattern of **1** with feature-to-feature spacing of 20 μm was produced by each tip in the array by pushing the tips into the SLG surface (SLG on 285 nm SiO<sub>2</sub>) at times ranging from 15 to 30 min and a force of ~100 mN at each spot.<sup>14</sup> The transfer of the **1**/PEG mixture into 2 × 3 patterns and an approach dot to level the arrays on the surface was confirmed by light microscopy (Figure 2a).

After the surfaces were washed with EtOH and H<sub>2</sub>O to remove unreacted **1** and PEG, the surface bonding was analyzed by Raman microscopy (WITec, 633 nm excitation). A Raman map of the surface that was obtained following force-accelerated printing of **1** revealed a 2 × 3 pattern of features where  $I_D$  was elevated significantly compared to surrounding areas (Figure 2b). The 20 μm spacing between features in the 2 × 3 patterns observed in the Raman map matched with the pattern of features printed by the pen array.<sup>18</sup> The elevated  $I_D$  was observed at all points where the tips were pressed into the surface for all dwell times above 15 min, but poor signal was obtained for dwell times below 12 min. Importantly, control experiments, where **1** was not present in the ink mixture or where **1** was present but force was not applied to the surface upon ink transfer, did not produce similar patterns or significantly elevated  $I_D/I_G$ , confirming that the diene and

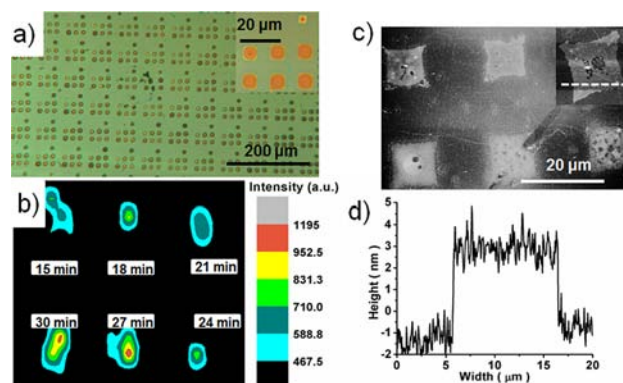


**Figure 2.** (a) Light microscopy image (10× magnification) of 2 × 3 dot arrays of a mixture containing **1** and PEG, with varying dwell times (30, 27, 24, 21, 18, 15 min), that were patterned by each pen in the tip array. Scale bar is 200 μm. Inset is a magnified image of one array. Scale bar is 20 μm. (b) Raman mapping image (1324 cm<sup>-1</sup>, D band) of 2 × 3 dot arrays of **1** covalently immobilized onto the SLG. Scale bar is 20 μm. (c) AFM image of a single feature printed onto the SLG. (d) Height profile of a single feature of **1** patterned onto SLG.

force are both necessary for changes in bonding to occur. AFM height images show the presence of elevated surfaces where the dienes had been printed (Figure 2c and 2d), with a height of ~3.5 nm, which is too high for a monolayer of **1**.

Spectra associated with different points on the Raman map confirmed that the changes in bonding were produced because of localized DA reactions (Figure 3). A Raman spectrum taken at a point where the inked tips were pressed into the surface had peaks of **1** and an increased  $I_D/I_G$  value of 0.56, compared to 0.14 for the unaltered surface, 0.17 where the tips had been pressed into the surface in the absence of **1**, and 0.16 for the original SLG surface.<sup>18</sup> Changes in the  $I_D/I_G$  indicate that the force-induced reaction of **1** with SLG converts some C–C bonds in the SLG from sp<sup>2</sup> to sp<sup>3</sup>, consistent with previous observations for DA reactions on SLG surfaces.<sup>8</sup>

Electrochemically active CP **2** was patterned onto SLG following a similar protocol described above, and the immobilization density of **2** on the SLG surface was analyzed by cyclic voltammetry (CV). Each tip in the pen array produced a 2 × 3 dot pattern over the 1 cm<sup>2</sup> area with an average feature edge length of 7.1 μm and area of 50.4 μm<sup>2</sup>. Following washing of the surface with EtOH and H<sub>2</sub>O to remove the PEG and unreacted **2**, CV was carried using a Ag/AgCl reference electrode, a Pt counter electrode, and the patterned SLG as the working electrode. A strong redox peak at  $E^0 = 590$  mV (vs Ag/AgCl) confirmed the presence of the ferrocene (fc)/ferrocenium (fc<sup>+</sup>) reversible redox couple from **2** (Figure 4), which is shifted anodically compared to fc because of the ester linking the fc to the CP. Control experiments where **2** was deposited without force did not result in any observable current corresponding to the fc/fc<sup>+</sup> redox couple after washing, confirming that force is necessary to induce the DA reaction under these conditions. The linear relationship between peak current and scan rate confirmed that **2** is immobilized on the SLG surface<sup>17,19</sup> but that the localized changes in bonding from sp<sup>2</sup> to sp<sup>3</sup> do not prevent conduction through the SLG. Interestingly, the increase in  $\Delta E$  with scan rate ( $\partial V/\partial t$ ) as well as the slope of 0.7 in the  $\ln(\partial V/\partial t)$  vs  $\ln(I)$ , indicates complexity in the charge transfer from the fc to the SLG. From integration of the CV, a charge density ( $\Gamma_{fc}$ ) of  $(5.34 \pm 0.76) \times 10^{14}$  cm<sup>-2</sup> was obtained,<sup>18</sup> which is significantly higher than

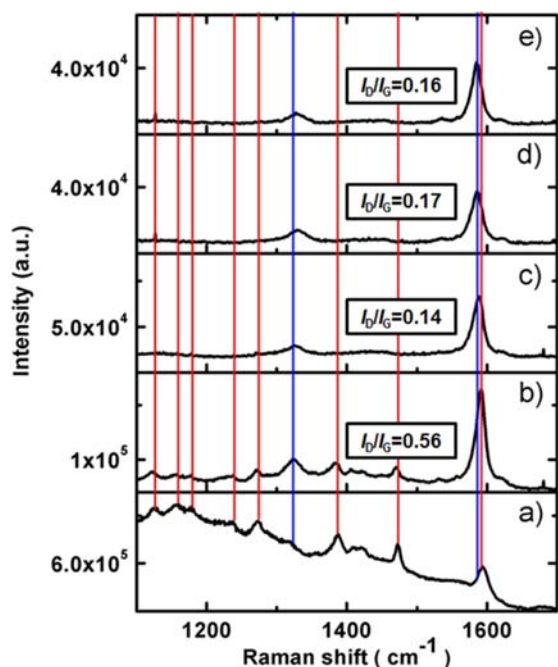


**Figure 3.** (a) Raman spectrum of **1** on a SiO<sub>2</sub> surface. (b) Raman spectrum from a map with force-accelerated printing of **1** (Figure 2b) taken at a position with increased D-band intensity ( $I_D$ ) compared to unreacted SLG also has peaks corresponding to **1**. (c) Raman spectrum from the map of the same printed surface taken at a position without increased  $I_D$ . (d) Raman spectrum of control experiment where PEG and force were applied to the SLG surface without **1**, taken at a point where the tips were pushed into the SLG surface. (e) Raman spectrum of pure SLG. Red lines mark peaks of **1** (11124, 1157, 1178, 1240, 1272, 1387, 1471, 1594 cm<sup>-1</sup>). Blue lines mark SLG peaks (1324, 1584 cm<sup>-1</sup>).

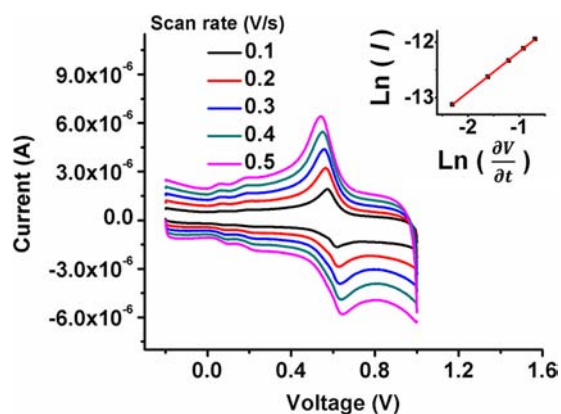


**Figure 4.** Cyclic voltammetry (CV) of **2** on SLG using a Pt counter electrode and Ag/AgCl reference electrode in 0.1 M HClO<sub>4</sub> electrolyte. (Inset) Relationship between  $\ln(\text{scan rate})$  and  $\ln(i_p/i_p^0)$ .

would be expected from the increase in the D-band intensity of the Raman spectrum.

To further study the reaction between CP and SLG as well as explain the CV and AFM results, DFT calculations were conducted for DA reactions of CP on three representative bonds in a 5 × 5 graphene model (Figure 5a). Hydrogen-substituted edges were used, although the nature of the edge is likely complex.<sup>2d,4</sup> The corner bond “a” can be viewed as the joint part of zigzag and armchair edges of graphene. Another

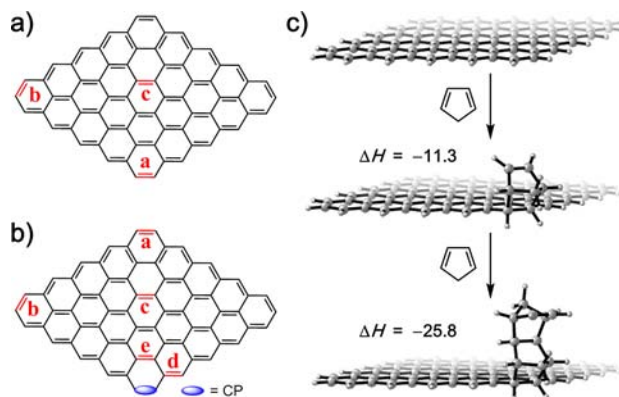


**Figure 5.** (a) 5 × 5 graphene model with the representative addition sites in red. (b) DA reaction sites of the second CP on graphene–CP cycloadduct. (c) Structures of graphene, graphene–CP cycloadduct, and the following CP dimerization product, reaction enthalpies in kcal/mol.

periphery bond “b” represents the edges, and the center bond “c” most resembles the pristine graphene interior. All structures were optimized at (U)M06-2X/6-31G(d) level, and single-point energy calculations were carried out on the optimized structures at the (U)M06-2X/6-311G(d,p) level.<sup>18</sup> We report here only the situation involving graphene acting as dienophile and CP as diene. Two more reaction pathways were also found to be unfavorable.<sup>18</sup>

Computational results (Table S1 in SI) show that the Diels–Alder cycloadditions at bonds “a” and “b” have reaction enthalpies of –11.3 and –1.4 kcal/mol, respectively. However, bond “c” involves unfavorable, endothermic enthalpy (36.6 kcal/mol) under standard conditions. The bond “c” most resembles the interior of pristine graphene. The thermochemical calculations of single CP on graphene demonstrate that center bonds cannot be functionalized through DA reactions with CPs, and only some special edges, comparable to defect sites, will be reactive. However, once the CP has been attached to the edge positions, it might either activate nearby bonds or itself react. The DA reaction of a second CP on the graphene–CP cycloadduct (functionalized on bond “a”) was also calculated (Figure 5b). Five additional bonds were evaluated (“a”, “b”, “c”, “d”, and “e”, Figure 5b). The new reaction enthalpies for the CP addition on bonds “a”, “b”, and “c” of the graphene–CP cycloadduct (Table S2 in SI) are practically unchanged. This clearly indicates that the functionalization at the edge bond “a” does not favor the subsequent CP addition on the graphene lattice. The reaction enthalpies on neighboring bonds “d” and “e” are 1.6 and 37.4 kcal/mol, respectively. Cycloaddition on bond “e” is impossible because of high endothermicity. Bond “d” can be viewed as the edge bond on a 4 × 4 graphene model and thus possesses a reactivity comparable to bond “a”. The enthalpy of 1.6 kcal/mol on bond “d” indicates that the CP group has in fact deactivated its nearby bonds by steric hindrance.

From CV data, we determine that approximately 1 fc is present on the surface for every 5 graphene double bonds, while calculations indicate that such a high coverage is not attainable because most of the graphene double bonds are unreactive with CP. How can the differences between experiment and computation be explained? Inspired by a recent report of the functionalization of graphene by polymerization,<sup>20</sup> we postulate that CP also oligomerizes through DA

reactions. Figure 5c shows structures of the graphene–CP cycloadduct and its CP dimerization product. The double bond of the graphene–CP cycloadduct resembles that of norbornene. The reaction enthalpy for the cycloaddition of a second CP is  $-25.8$  kcal/mol. This is significantly more exothermic than any of the reactions of graphene calculated above (the most reactive site on graphene model is bond “a” with  $\Delta H$  of  $-11.3$  kcal/mol). Once one CP reacts with a reactive edge or defect on graphene, the second CP can react with the norbornene double bond. This can be repeated because CP is well-known to dimerize and polymerize through DA reactions.<sup>21</sup> Oligomerization of CP induced by an initial Diels–Alder reaction at a graphene defect is preferred over multisite functionalization. On the basis of the CV characterization and feature height of 3.5 nm, which would correspond to a degree of CP oligomerization of 15,<sup>18</sup> the functionalization degree of graphene is about 1.3%. Finally, the dependence of  $\Delta E$  with scan rate of the CV and the slope of 0.7 in the inset of Figure 4 can be attributed to hopping of electrons through the fc chains appended to the CP oligomers.

In conclusion, SLG sheets on SiO<sub>2</sub> substrates have been patterned covalently with oligomers of organic small molecules through a force-accelerated DA reaction induced on graphene defect and edge sites by an array of pyramidal elastomeric tips. The changes in bonding were characterized by Raman microscopy, cyclic voltammetry, and electronic structure calculations, and the results are consistent with micrometer-scale features composed of covalently immobilized molecules patterned over large (cm<sup>2</sup>) areas. Importantly, these reactions occur at ambient temperature and atmosphere, while accessing one of the most versatile reactions in organic chemistry. Future studies will extend this method to other reactions that are accelerated by force, and elucidate the role of force on reaction rate, reversibility, and regioselectivity. This method for functionalizing the basal plane of graphene, while maintaining the conductivity of the surface, could find utility in sensors, electronics, and optical devices.

## ■ ASSOCIATED CONTENT

### Supporting Information

Organic synthesis, microfabrication and lithography, Raman and electrochemical characterization, control experiments, computational details, and cartesian coordinates of all analyzed structures. This material is available free of charge via the Internet at <http://pubs.acs.org>.

## ■ AUTHOR INFORMATION

### Corresponding Author

a.braunschweig@miami.edu; houk@chem.ucla.edu

### Notes

The authors declare no competing financial interest.

## ■ ACKNOWLEDGMENTS

A.B.B. is grateful to the Air Force Office of Scientific Research (Young Investigator Award FA9550-11-1-0032) and the National Science Foundation (DBI-115269) for generous support, Prof. Chad A. Mirkin for use of the Raman microscope, and Prof. A. E. Kaifer for helpful discussions. K.N.H. is grateful to the National Science Foundation (CHE-1059084) for financial support. S.O. acknowledges the European Community for the postdoctoral fellowship (PIOF-GA-2009-252856). Calculations were performed on the

Hoffman2 Cluster at UCLA and the Extreme Science and Engineering Discovery Environment (XSEDE), which is supported by the NSF (OCI-1053575).

## ■ REFERENCES

- (1) Novoselov, K. S.; Geim, A. K.; Morozov, S. V.; Jiang, D.; Zhang, Y.; Dubonos, S. V.; Grigorieva, I. V.; Firsov, A. A. *Science* **2004**, *306*, 666.
- (2) (a) Lin, Y. M.; Dimitrakopoulos, C.; Jenkins, K. A.; Farmer, D. B.; Chiu, H. Y.; Grill, A.; Avouris, P. *Science* **2010**, *327*, 662. (b) Wang, Q. H.; Jin, Z.; Kim, K. K.; Hilmer, A. J.; Paulus, G. L. C.; Shih, C. J.; Ham, M. H.; Sanchez-Yamagishi, J. D.; Watanabe, K.; Taniguchi, T.; Kong, J.; Jarillo-Herrero, P.; Strano, M. S. *Nat. Chem.* **2012**, *4*, 724. (c) Rodriguez-Lopez, J.; Ritzert, N. L.; Mann, J. A.; Tan, C.; Dichtel, W. R.; Abruna, H. D. *J. Am. Chem. Soc.* **2012**, *134*, 6224. (d) Kim, S. N.; Kuang, Z. F.; Slocik, J. M.; Jones, S. E.; Cui, Y.; Farmer, B. L.; McAlpine, M. C.; Naik, R. R. *J. Am. Chem. Soc.* **2011**, *133*, 14480. (e) Ragoussi, M. E.; Malig, J.; Katsukis, G.; Butz, B.; Spiecker, E.; de la Torre, G.; Torres, T.; Guldi, D. M. *Angew. Chem., Int. Ed.* **2012**, *51*, 6421. (f) Liu, M.; Yin, X. B.; Ulin-Avila, E.; Geng, B. S.; Zentgraf, T.; Ju, L.; Wang, F.; Zhang, X. *Nature* **2011**, *474*, 64.
- (3) (a) Lee, B.; Chen, Y.; Duerr, F.; Mastrogianni, D.; Garfunkel, E.; Andrei, E. Y.; Podzorov, V. *Nano Lett.* **2010**, *10*, 2427. (b) Zhou, X.; He, S.; Brown, K. A.; Mendez-Arroyo, J.; Boey, F.; Mirkin, C. A. *Nano Lett.* **2013**, *13*, 1616.
- (4) Steenackers, M.; Gigler, A. M.; Zhang, N.; Deubel, F.; Seifert, M.; Hess, L. H.; Lim, C. H. Y. X.; Loh, K. P.; Garrido, J. A.; Jordan, R.; Stutzmann, M.; Sharp, I. D. *J. Am. Chem. Soc.* **2011**, *133*, 10490.
- (5) Liu, H. T.; Ryu, S. M.; Chen, Z. Y.; Steigerwald, M. L.; Nuckolls, C.; Brus, L. E. *J. Am. Chem. Soc.* **2009**, *131*, 17099.
- (6) Quintana, M.; Spyrou, K.; Grzelczak, M.; Browne, W. R.; Rudolf, P.; Prato, M. *ACS Nano* **2010**, *4*, 3527.
- (7) (a) Bekyarova, E.; Itkis, M. E.; Ramesh, P.; Berger, C.; Sprinkle, M.; De Heer, W. A.; Haddon, R. C. *J. Am. Chem. Soc.* **2009**, *131*, 1336. (b) Georgakilas, V.; Bourlinos, A. B.; Zboril, R.; Steriotis, T. A.; Dallas, P.; Stubos, A. K.; Trapalis, C. *Chem. Commun.* **2010**, *46*, 1766. (c) Lomeda, J. R.; Doyle, C. D.; Kosynkin, D. V.; Hwang, W. F.; Tour, J. M. *J. Am. Chem. Soc.* **2008**, *130*, 16201. (d) Hossain, M. Z.; Walsh, M. A.; Hersam, M. C. *J. Am. Chem. Soc.* **2010**, *132*, 15399.
- (8) (a) Sarkar, S.; Bekyarova, E.; Niyogi, S.; Haddon, R. C. *J. Am. Chem. Soc.* **2011**, *133*, 3324. (b) Sarkar, S.; Bekyarova, E.; Haddon, R. C. *Acc. Chem. Res.* **2012**, *45*, 673.
- (9) (a) van Eldik, R.; Asano, T.; le Noble, W. J. *Chem. Rev.* **1989**, *89*, 549. (b) Kuster, C. J. T.; Scheeren, H. W. In *High Pressure Chemistry*; van Eldik, R., Klaerner, F.-G., Eds.; Wiley-VCH: Weinheim, 2007; pp284–304.
- (10) (a) Rozkiewicz, D. I.; Janczewski, D.; Verboom, W.; Ravoo, B. J.; Reinhoudt, D. N. *Angew. Chem., Int. Ed.* **2006**, *45*, 5292. (b) Mehlich, J.; Ravoo, B. *J. Org. Biomol. Chem.* **2011**, *9*, 4108.
- (11) Huo, F.; Zheng, Z.; Zheng, G.; Giam, L. R.; Zhang, H.; Mirkin, C. A. *Science* **2008**, *321*, 1658.
- (12) Bian, S.; He, J.; Schesing, K. B.; Braunschweig, A. B. *Small* **2012**, *8*, 2000.
- (13) Bian, S. D.; Schesing, K. B.; Braunschweig, A. B. *Chem. Commun.* **2012**, *48*, 4995.
- (14) Liao, X.; Braunschweig, A. B.; Zheng, Z. J.; Mirkin, C. A. *Small* **2010**, *6*, 1082.
- (15) Yousaf, M. N.; Mrksich, M. *J. Am. Chem. Soc.* **1999**, *121*, 4286.
- (16) Cancado, L. G.; Jorio, A.; Ferreira, E. H. M.; Stavale, F.; Achete, C. A.; Capaz, R. B.; Moutinho, M. V. O.; Lombardo, A.; Kulmala, T. S.; Ferrari, A. C. *Nano Lett.* **2011**, *11*, 3190.
- (17) Bard, A. J.; Faulkner, L. R. *Electrochemical Methods: Fundamentals and Applications*, 2nd ed.; Wiley: New York, 2001.
- (18) See Supporting Information for details.
- (19) Chidsey, C. E. D.; Bertozzi, C. R.; Putvinski, T. M.; Mujsce, A. M. *J. Am. Chem. Soc.* **1990**, *112*, 4301.
- (20) Ma, X.; Li, F.; Wang, Y.; Hu, A. *Chem.—Asian J.* **2012**, *7*, 2547.
- (21) Alder, K.; Stein, G. *Justus Liebigs Ann. Chem.* **1933**, *504*, 216.